UV ABSORPTION CROSS SECTIONS OF HO_2NO_2 VAPOR

LUISA T. MOLINA and MARIO J. MOLINA
Department of Chemistry, University of California, Irvine, CA 92717 (U.S.A.)
(Received September 1, 1980)

Summary

The UV absorption cross sections for gas phase pernitric acid (HO_2NO_2) were measured between 190 and 330 nm at 298 K and 1 atm total pressure. The HO_2NO_2 vapor was prepared in a flowing stream of nitrogen in the presence of H_2O, H_2O_2, HNO_3 and NO_2. The composition of the mixture was established by visible and IR absorption spectroscopy and by chemical titration after absorption in aqueous solutions. The HO_2NO_2 cross sections ranged from approximately 10^{-17} cm^2 molecule^{-1} at 190 nm to about 10^{-21} cm^2 molecule^{-1} at 330 nm. The experimental uncertainty (one standard deviation) ranged from 5% at 200 nm to 30% at 330 nm and fell mainly in the 10% range. The solar photodissociation rate in the troposphere and lower stratosphere was estimated to be about 10^{-5} s^{-1} for a solar zenith angle of 0°.

1. Introduction

Pernitric acid (also called peroxynitric acid, HO_2NO_2) is formed in the atmosphere by the recombination of HO_2 and NO_2 radicals:

$$HO_2 + NO_2 \xrightarrow{M} HO_2NO_2 \quad (1)$$

This reaction was proposed, among others, by Johnston [1] but it received little attention until Niki *et al.* [2] identified HO_2NO_2 for the first time in the gas phase through Fourier-transform IR spectroscopy; Hanst and Gay [3] and Levine *et al.* [4] further corroborated the findings of Niki *et al.* In fact, HO_2NO_2 was first characterized by Schwarz [5] in liquid solutions through its strongly oxidizing properties, *i.e.* the release of Br_2 from KBr solutions.

The importance of HO_2NO_2 is now well established; the potential role of this species for stratospheric chemistry has been discussed, for example, by Jesson *et al.* [6] and by Graham *et al.* [7, 8].

Howard [9] has measured the rate constant for reaction (1), and the HO_2NO_2 thermal decomposition rate, the reverse of reaction (1), has been studied by Graham *et al.* [7]:

0047-2670/81/0000-0000/$02.50

$$HO_2NO_2 \xrightarrow{M} HO_2 + NO_2 \quad (2)$$

In the atmosphere HO_2NO_2 may be destroyed by reaction (2), by reaction with OH radicals (reaction 3) or by photolysis (reaction 4):

$$HO_2NO_2 + OH \rightarrow H_2O + O_2 + NO_2 \quad (3)$$

$$HO_2NO_2 + h\nu \rightarrow \text{products} \quad (4)$$

Photolysis is likely to be an important atmospheric sink [6, 8]. An upper limit of 3×10^{-12} cm^3 $molecule^{-1}$ s^{-1} for the rate constant for reaction (3) has been established by Graham *et al.* [7] and by Trevor *et al.* [10]. Reaction with oxygen atoms and chlorine atoms is also possible, but almost certainly of little importance in the stratosphere.

There are now four studies of the UV spectrum of HO_2NO_2: Jesson *et al.* [6] have measured the spectra of equilibrium mixtures of HNO_3, H_2O_2 and HO_2NO_2 in concentrated aqueous solution between 300 and 360 nm; Cox and Patrick [11] and Morel *et al.* [12], both using a static photochemical system containing HO_2NO_2 vapor, have obtained absorption cross sections in the ranges 195 - 265 nm and 200 - 290 nm respectively; there is, however, only one study, that of Graham *et al.* [8], of the HO_2NO_2 gas phase spectrum covering the critical wavelength range for atmospheric photodissociation, *i.e.* wavelengths longer than 290 nm. Graham *et al.* have prepared HO_2NO_2 vapor in a static system at a concentration of a few millitorr, and their cross section values are about a factor of 5 larger than those of Jesson *et al.*

We report in this work measurements of the absorption cross sections of HO_2NO_2 vapor in the 190 - 330 nm region. HO_2NO_2 was prepared in a flow system at concentrations approaching 1 Torr, in the presence of 1 atm N_2 and of NO_2, H_2O_2, H_2O and HNO_3 in the subtorr range. The composition of the mixture was established by Fourier-transform IR spectroscopy, by chemical titration of the flowing gas after absorption in aqueous solutions and by the absorption spectrum in the visible.

2. Experimental

2.1. Instrumentation

The UV and visible (VIS) spectra were recorded with a Cary 219 double-beam spectrophotometer interfaced to a Nova 3 computer equipped with a 10 megabyte storage disk, a Tektronix 4006-1 display terminal and a Versatec 1200A printer–plotter. Two quartz absorption cells fused with Suprasil windows were used: one 10 cm long and 2.5 cm in diameter and the other 90 cm long and 3.5 cm in diameter with folded optics to give an optical path length of 180 cm. The Cary 219 spectrophotometer has a limiting resolution of 0.07 nm and is capable of measuring reproducibly absorbances in the range 0.002 - 4. To achieve rapid data collection the present study

used a sampling rate of 10 Hz and a scan rate of 1 nm s^{-1} with a spectral bandwidth of 0.1 - 0.2 nm in the long wavelength region (500 - 300 nm) and of 0.3 - 0.5 nm at wavelengths below 300 nm. A total of about 100 spectral files (HO_2NO_2, H_2O_2, HNO_3, NO_2 and background spectra) consisting typically of 3000 data points each were recorded and were stored in the computer for later manipulations.

A Digilab FTS-12A Fourier-transform IR (FT–IR) spectrometer equipped with a standard Digilab data-handling system and a liquid-nitrogen-cooled HgCdTe detector was employed for the IR analysis. A Pyrex absorption cell, 50 cm long, 2.5 cm in diameter and fitted with germanium windows, was used in the single-pass mode. The spectra were taken at a resolution of 1 cm^{-1} and each spectrum was computed from the average of 64 interferograms. About 100 FT–IR spectra were recorded simultaneously with the UV–VIS spectra. The concentrations of the various components of each mixture were obtained by subtraction of reference spectra.

2.2. Synthesis of HO_2NO_2

Two methods were used to prepare HO_2NO_2. The first was a modification of the original method of Schwarz [5]. HO_2NO_2 was generated continuously by mixing 70% HNO_3 with 90% H_2O_2 in a porous glass bubbler. The HO_2NO_2 vapor was carried by a stream of nitrogen gas which was forced through the bubbler into the absorption cells. The bubbler was immersed in a water bath maintained at constant temperature to within 0.2 °C while the absorption cells remained at room temperature (25 °C). This method produced typically about 0.5 Torr HO_2NO_2 in the presence of approximately 1 Torr HNO_3 and about 0.1 Torr H_2O_2. A small amount of NO_2 (about 0.05 Torr) was also present. Once the cells had been conditioned, the concentration of HO_2NO_2 could be maintained constant over a period of 1 - 2 h.

The second technique employed nitronium tetrafluoroborate (NO_2BF_4) rather than HNO_3 as the nitrating agent [13]. Solid NO_2BF_4 was slowly added to a solution of 90% H_2O_2 which was stirred with a magnetic stirring bar at 0 °C. This preparation was carried out in a nitrogen atmosphere glove cabinet because of the hygroscopic nature of NO_2BF_4. The final solution was then transferred to the glass bubbler as in the first method. This technique produced a very high concentration of HO_2NO_2 vapor (approximately 1 - 2 Torr) in the presence of small amounts of HNO_3 (about 0.2 Torr), H_2O_2 (about 0.5 Torr) and NO_2 (about 0.05 Torr), but it had the disadvantage that the HO_2NO_2 was formed all at once at the beginning and its concentration decreased rapidly during the course of the experiment. A small amount of HF, detected indirectly in the IR as SiF_4 (below 0.05 Torr), was also generated in this system. These two techniques provided independent means of deducing the absorption spectra of HO_2NO_2 from chemical titrations and spectral analyses of mixtures containing widely different concentrations of HO_2NO_2, HNO_3 and H_2O_2.

After flowing the mixture through the cell for 10 - 30 min, the first UV and IR spectra were measured; successive spectra were recorded every 10

min and chemical titrations were carried out at 2 min intervals. The average residence times of the flowing gaseous mixture were about 30 s in the IR cell, 100 s in the 90 cm UV cell and 4 s in the 10 cm UV cell.

NO_2 (99.5%, Matheson Gas Products), H_2O_2 (90%, FMC Corporation) and HNO_3 (70%, Mallinckrodt) were used without further purification.

2.3. Chemical titration and spectral analysis

The reference spectra employed for spectral subtractions were obtained by introducing each sample individually into the UV and IR cells. The absorption spectra of about 0.05 - 0.5 Torr of NO_2 in nitrogen (total pressure, 1 atm) were recorded by introducing the mixture into the absorption cells using a greaseless vacuum line. All pressure measurements were carried out with two MKS capacitance manometers (ranges of 0 - 10 Torr and 0 - 1000 Torr). The procedure used in the absorption measurements of H_2O_2 has been described previously [14]. Briefly, nitrogen gas was forced through a bubbler containing concentrated H_2O_2 solution, the concentration of H_2O_2 in the nitrogen carrier gas being determined by bubbling the gas through a measured volume of standard $KMnO_4$ solution. The gas phase concentration of H_2O_2 was controlled by varying the temperature of the bubbler between 8 and 18 °C. Titration of the gaseous stream before and after passage through the cells (connected in series, from IR to UV or from UV to IR) indicated that after an initial conditioning period less than 10% of the H_2O_2 decomposed in the cells. A similar flow technique was employed in the spectral measurements of HNO_3. In this case the concentration of HNO_3 in the nitrogen carrier gas was determined by titration with standard NaOH solution and the concentration of HNO_3 vapor was controlled by varying the bubbler temperature between 3 and 16 °C.

The concentration of HO_2NO_2 in the nitrogen carrier gas was determined by bubbling the gas through a measured volume of KBr solution and by measuring spectrophotometrically the Br_2 liberated. Usually it took 30 - 60 s to observe an absorbance of 0.5. A Hitachi Perkin–Elmer 139 UV–VIS spectrophotometer was used for this measurement. The amount of Br_2 was determined by comparing the measured absorbance at 417 nm with a calibration curve obtained from standard $KBrO_3$–KBr solutions. Control experiments showed that H_2O_2 or HNO_3 alone do not oxidize KBr. Furthermore, when H_2O_2 and HNO_3 were placed in two separate bubblers and the gaseous streams from the two bubblers (with nitrogen carrier gas) were introduced into a solution of KBr, it took about ten times longer to observe a noticeable color change. A second independent determination of the HO_2NO_2 concentration was provided by titration with standard NaOH solution. The total acidity measured was the sum of the acidities of HNO_3, NO_2 and HO_2NO_2. After correcting for HNO_3 and NO_2 the calculated pressure of HO_2NO_2 agreed with that obtained from the KBr analysis. The concentrations of H_2O_2 and HNO_3 in the HO_2NO_2 sample were determined from the IR spectral analysis and the NO_2 concentration was measured from its structured spectrum in the 400 - 500 nm region.

3. Results and discussion

3.1. HNO_3, H_2O_2 and NO_2 spectra

The UV absorption spectra of 10 samples of H_2O_2 and 15 samples of HNO_3 were measured using the flow technique and chemical titration. The results are shown in Figs. 1 and 2 and Table 1. The absorption cross sections for HNO_3 are in very good agreement with the measurements of Johnston and Graham [15] except at both ends of the spectrum. In fact, Biaume [16] has observed the same discrepancies in these two regions, and our values agree better with those reported by Biaume. In the case of H_2O_2, although our present values are slightly lower than both our earlier results [14] and those reported by Lin *et al.* [17], they fall within the experimental uncertainties cited in these earlier studies.

The UV–VIS absorption spectra of NO_2 over the pressure range 0.05 - 0.5 Torr were stored in the computer and were used to correct the HO_2NO_2 spectra for the NO_2 contribution. The amount of NO_2 was determined from its structured spectrum between 400 and 500 nm, and it was found to be less than 0.05 Torr in most cases. The maximum amount of N_2O_4 present under these conditions can be calculated to be less than 1% of the NO_2 present.

3.2. HO_2NO_2 spectra

Some typical IR and UV–VIS spectra of an HO_2NO_2–HNO_3–H_2O_2–NO_2 mixture prepared by the first of the two techniques described in Section 2.2 are shown in Figs. 3 and 4. In Fig. 4 the 500 - 280 nm and 340 - 250 nm spectra were taken with a cell of path length 180 cm while the 260 -

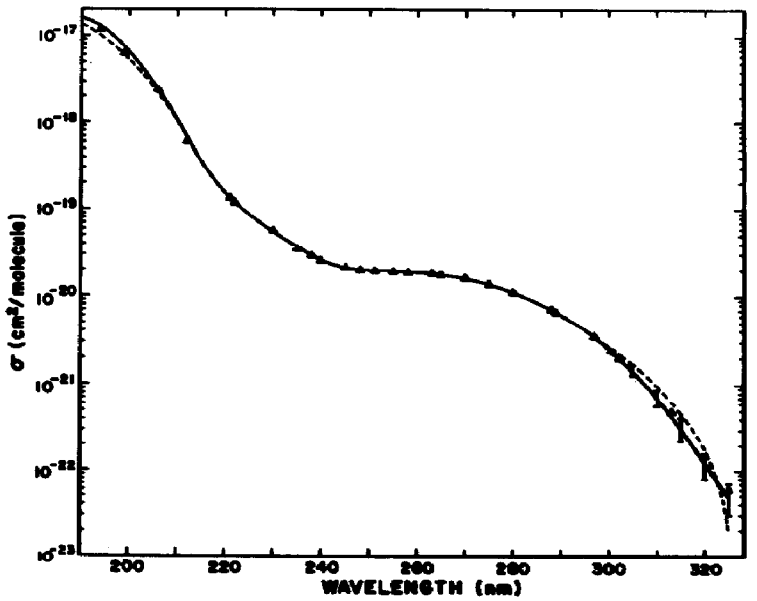

Fig. 1. The UV spectrum of HNO_3 vapor: ——, this work; — — —, from ref. 15; △, from ref. 16.

TABLE 1

Absorption cross sections of HNO_3 and H_2O_2

λ (nm)	σ (×10^{20} cm^2 molecule^{-1})	
	HNO_3	H_2O_2
190	1560	67.2
195	1150	56.2
200	661	46.7
205	293	39.5
210	105	33.6
215	35.6	28.7
220	15.1	24.5
225	8.62	20.6
230	5.66	17.1
235	3.72	14.0
240	2.57	11.5
245	2.10	9.42
250	1.91	7.69
255	1.90	6.23
260	1.88	4.94
265	1.71	3.86
270	1.59	3.11
275	1.35	2.42
280	1.10	1.87
285	0.848	1.46
290	0.607	1.12
295	0.409	0.870
300	0.241	0.663
305	0.146	0.493
310	0.071	0.364
315	0.032	0.280
320	0.012	0.200
325	0.005	0.140
330	0.002	0.105
335		0.078
340		0.055
345		0.04
350		0.03

200 nm spectra were taken with a 10 cm cell. As can be seen in Fig. 4, the absorption in the visible is due entirely to NO_2 whereas HNO_3 is responsible for most of the absorption for wavelengths below 210 nm.

The IR absorption cross sections of HO_2NO_2 at a resolution of 1 cm^{-1} and 1 atm total pressure are given in Table 2. These were obtained from the spectra of the gaseous mixtures after subtraction of the HNO_3 and H_2O_2 contributions. The HO_2NO_2 pressures were determined from KBr titrations and ranged from 0.2 to 1.0 Torr. Beer's law was shown to hold for the P, Q and R branches of the four absorption bands. As can be seen in Table 2, our absorption cross sections for the 810 - 814 cm^{-1} R branch and the 1295 -

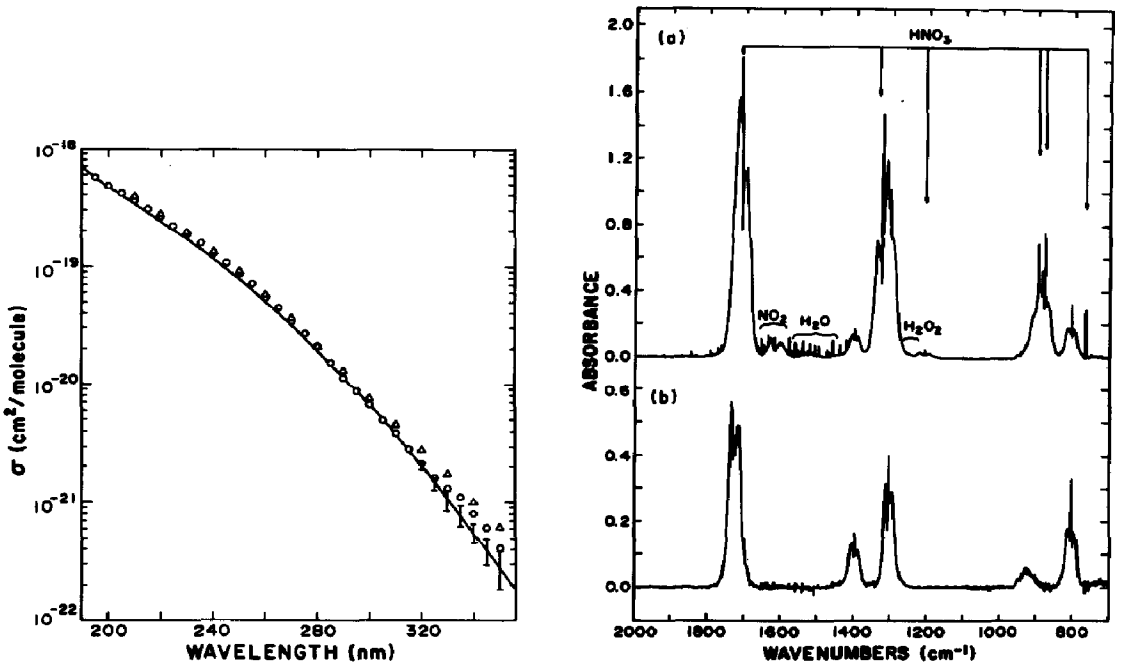

Fig. 2. The UV spectrum of H_2O_2 vapor: ——, this work; ○, from ref. 17; △, from ref. 14.

Fig. 3. Typical IR spectra of a mixture containing HO_2NO_2 formed via $H_2O_2 + HNO_3$: (a) product spectrum from $H_2O_2 + HNO_3$ reaction; (b) residual spectrum (HO_2NO_2) after subtraction of HNO_3, H_2O_2, NO_2 and H_2O.

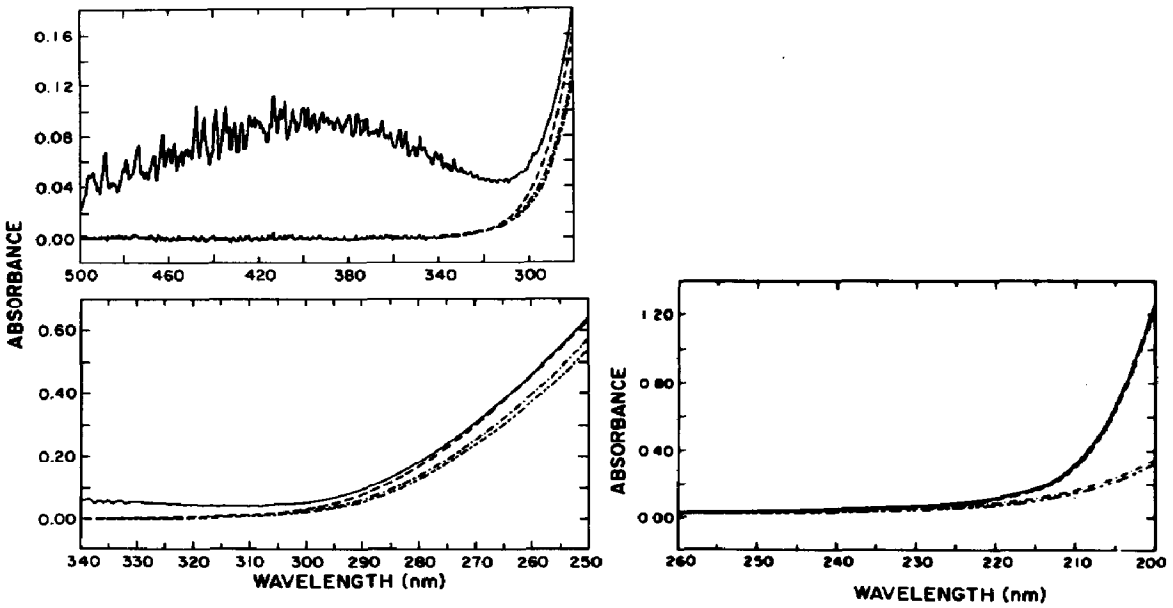

Fig. 4. Typical UV–VIS spectra of a mixture containing HO_2NO_2 formed via $H_2O_2 + HNO_3$: ——, original spectrum; — — —, original spectrum after correcting for NO_2; — · — · —, previous spectrum after correcting for HNO_3; — · · · —, previous spectrum after correcting for H_2O_2.

TABLE 2

IR absorption cross sections of HO_2NO_2 at a resolution of 1 cm^{-1}

ν (cm^{-1})	σ ($\times 10^{18}$ cm^2 $molecule^{-1}$)	
	This work[a]	*Graham et al.* [8][b]
802.7 (Q)	1.0	1.5
1304.2 (Q)	1.3	1.6
1396.9 (Q)	0.54	0.6
1728.3 (Q)	1.4	1.7
810 - 814 (R)	0.56	0.56
1295 - 1296 (P)	0.90	1.0

[a]Total pressure, 1 atm.
[b]Total pressure, 1 - 20 Torr.

1296 cm^{-1} P branch are in good agreement with those reported by Graham *et al.* [8] while those for the Q branches are lower; this is probably due to pressure-broadening effects. We did not include the cross sections for the 3540 cm^{-1} band because of the relatively low signal-to-noise ratio arising from the weak response of our detector in that spectral region.

The UV absorption cross sections of HO_2NO_2 vapor at 298 K are presented in Table 3 and Fig. 5; the cross section values reported by other workers are also included for comparison. Our results are based on spectra of approximately 60 gaseous samples of HO_2NO_2 prepared by the two different methods described in Section 2.2 and using three different flow rates. Some spectra were taken with the HO_2NO_2 sample flowing through the UV cell followed by the IR cell, and some were recorded with the two cells in reverse order. Beer's law was obeyed throughout the HO_2NO_2 pressure range used in our absorption measurements, *i.e.* 0.2 - 1.0 Torr. The standard deviation was about 10% around 190 nm, 5% in the 200 - 270 nm range and it increased to about 30% at 330 nm.

3.3. Chemical kinetic considerations

The average residence time of the flowing gaseous mixture in our experiments was of the order of 1 min (see Section 2.2), while the HO_2NO_2 thermal decomposition lifetime is approximately 10 s at room temperature and 1 atm pressure [7, 11]. However, the NO_2–HO_2 recombination reaction is sufficiently rapid to keep the net rate of homogeneous gas phase decomposition at a negligible level under our experimental conditions, even considering the relatively fast disproportionation of the HO_2 radicals:

$$\frac{1}{[HO_2NO_2]} \frac{d[HO_2NO_2]}{dt} \approx 2k_3 \frac{k_2}{k_1} \frac{[HO_2NO_2]^2}{[NO_2]} \lesssim 0.05\% \text{ min}^{-1}$$

$$HO_2NO_2 \xrightarrow{M} HO_2 + NO_2 \qquad (5)$$

TABLE 3

Absorption cross sections of HO_2NO_2 vapor

λ (nm)	σ (×10^{20} cm^2 molecule^{-1})				
	This work	*Cox and Patrick* [11]	*Graham et al.* [8]	*Morel et al.* [12]	*Jesson et al.* [6][a]
190	1010		1610		
195	816	404	960		
200	563	434	640	435	
205	367	420	430	382	
210	241	378	290	289	
215	164	298	200	232	
220	120	220	154	164	
225	95.2	163	123	121	
230	80.8	120	99	97	
235	69.8	93	82	86	
240	59.1	76	68	74	
245	49.7	65	58	61	
250	41.8	54	51	52	
255	35.1	44	45	40	
260	27.8	30	40	34	
265	22.4	<10	35	27	
270	17.8		28	23	
275	13.4		23	15	
280	9.3		18	12	
285	6.3		14	10	
290	4.0		11	5	
295	2.6		8.4		
300	1.6		6.2		1.4
305	1.1		5.0		
310	0.7		4.2		0.92
315	0.4		3.6		
320	0.3		3.0		0.59
325	0.2		2.6		
330	0.1		2.2		0.1
340					0.01
350					0.0037
360					0.0016

[a] Aqueous solution.

$$HO_2 + NO_2 \xrightarrow{M} HO_2NO_2 \quad (6)$$

$$HO_2 + HO_2 \longrightarrow H_2O_2 + O_2 \quad (7)$$

We observed considerably larger decomposition rates, up to 5% min^{-1}, presumably because of heterogeneous processes. The procedure employed in our experiment was designed to minimize the latter processes: in addition to a small germanium surface, only glass and Teflon surfaces were present; the flowing mixture conditioned these surfaces and replenished the components of interest, thus eliminating the accumulation of impurities. The relatively

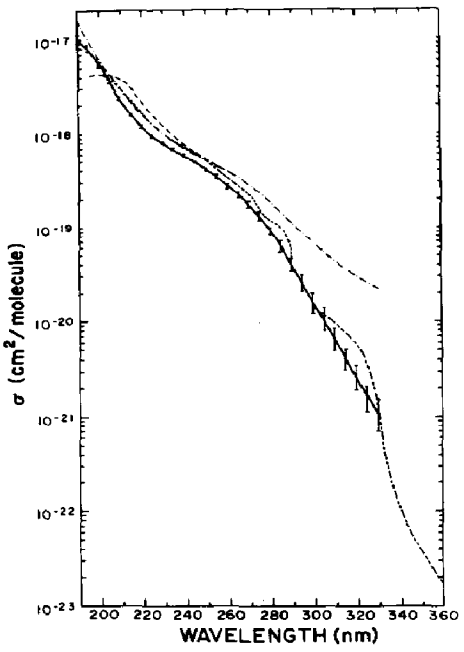

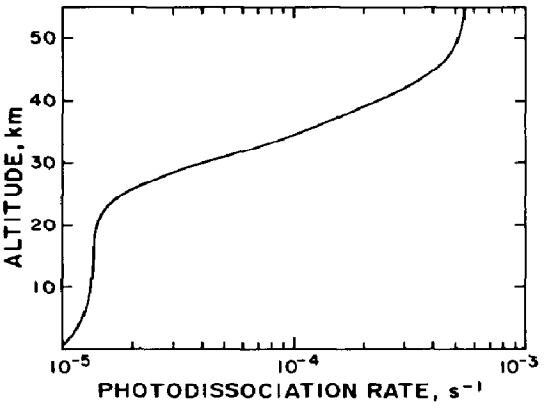

Fig. 5. The UV spectrum of HO_2NO_2 vapor: ——, this work; - - -, from ref. 12; — — —, from ref. 11; — · — · —, from ref. 8; — · · —, from ref. 6, aqueous solution.

Fig. 6. The atmospheric photodissociation rate of HO_2NO_2.

high pressure (1 atm N_2) of the inert carrier gas also slowed down diffusion to the walls.

3.4. Comparison with other measurements

Our measured UV absorption cross sections are in reasonable agreement with those reported by Graham *et al.* [8] except in the critical wavelength range for atmospheric photodissociation, *i.e.* 290 - 330 nm, where our numbers are about an order of magnitude smaller (see Fig. 5). The maximum HO_2NO_2 concentration was approximately 50 times larger and the maximum optical path length approximately 10 times smaller in our work. Thus, the net absorbance due to HO_2NO_2 should be up to 5 times greater in our UV cell. The discrepancy is well outside the limits of experimental error: the presence of unidentified impurities in our system can only increase the apparent HO_2NO_2 cross sections and we estimate an error of at most 50% from oversubtraction of absorbance due to NO_2, HNO_3 or H_2O_2. We can only speculate that some trace impurity might have been present in the work of Graham *et al.*, or the NO_2 absorbance was not subtracted with sufficient accuracy or perhaps they had complications with the UV instrumentation: a single-beam, single-monochromator and multiple-path UV spectrometer does not easily attain the extreme baseline stability required for absorbance measurements in the 0.005 - 0.02 range.

Our HO_2NO_2 cross section values differ somewhat from those reported by Jesson *et al.* [6] (see Fig. 5), but fall within their large estimated uncer-

tainty. As may be seen in the figure, our cross section values are in fair agreement with those of Cox and Patrick [11] and of Morel *et al.* [12], although our experimental uncertainty is not large enough to accommodate their values. However, these two sets of results were obtained through a measurement of the UV spectrum of static photolysis mixtures containing small amounts of HO_2NO_2 and containing many additional components, including Cl_2 and O_3. The composition of these complex mixtures was inferred solely from the UV spectrum itself and from kinetic considerations, and no IR or other chemical analysis was attempted; thus, we believe that the uncertainty in the work we report here is considerably smaller.

3.5. Atmospheric photodissociation rate

Figure 6 shows the atmospheric photodissociation rate of HO_2NO_2 as a function of altitude calculated with the cross section values presented in Table 1 and using the Lawrence Livermore Laboratory 1-D atmospheric photochemistry model [18]. The photodissociation rate in the troposphere is $J \approx 10^{-5}\ s^{-1}$, which corresponds to a lifetime $1/J$ of the order of 1 day. This lifetime might be actually longer in the lower stratosphere because of the lower temperatures prevailing at those altitudes: the cross sections in the wing of an absorption band often decrease with temperature. In the upper stratosphere photolysis will occur much more rapidly and predominantly with radiation in the 200 nm window.

The photodissociation rate calculation assumes unit quantum yield for photodecomposition, as expected from the continuous nature of the HO_2-NO_2 absorption spectrum. Also, the calculated rate includes only contributions from wavelengths shorter than 330 nm, since we were unable to measure absorption cross sections beyond this wavelength. The calculated photodissociation rate in the troposphere increases by about 30% if the absorption cross sections beyond 330 nm are computed by extrapolation: the logarithm of the absorption cross sections between 280 and 330 nm changes linearly with wavelength, as can be seen in Fig. 5.

Our experiments provide no information on the identity of the primary photolysis products: oxygen atoms, OH and HO_2 radicals are plausible species. This identity is likely to have little effect on predicted HO_2NO_2 profiles [6], but might play some role in overall NO_x chemistry at altitudes where HO_2NO_2 photodissociates rapidly.

Acknowledgments

This research was supported by the Department of Transportation, High Altitude Pollution Program, under Contract DOT-FA 78WA-4228. Also, we gratefully acknowledge the Environmental Protection Agency for the loan of the Digilab Fourier-transform spectrometer, under Grant EPA-R805532010.

We wish to thank Dr. Richard Hunter for his assistance in the construction of the computer interface to the UV spectrophotometer and Thao Duong for her assistance in the chemical titrations.

References

1 H. Johnston, Laboratory chemical kinetics as an atmospheric science. In A. E. Barrington (ed.), *Climatic Impact Assessment Program Proc. of the Survey Conf., February 1972; Final Rep. DOT-TSC-OST-72-13*, Springfield, Virginia, September 1972.
2 H. Niki, P. D. Maker, C. M. Savage and L. P. Breitenbach, *Chem. Phys. Lett., 45* (1977) 564.
3 P. L. Hanst and B. W. Gay, Jr., *Environ. Sci. Technol., 11* (1977) 1105.
4 S. Z. Levine, W. M. Uselman, W. H. Chan, J. G. Calvert and J. H. Shaw, *Chem. Phys. Lett., 48* (1977) 528.
5 R. Schwarz, *Z. Anorg. Chem., 256* (1948) 3.
6 J. P. Jesson, L. P. Glasgow, D. L. Filkin and C. Miller, *Geophys. Res. Lett., 4* (1977) 513.
7 R. A. Graham, A. M. Winer and J. N. Pitts, Jr., *J. Chem. Phys., 68* (1978) 4505.
8 R. A. Graham, A. M. Winer and J. N. Pitts, Jr., *Geophys. Res. Lett., 5* (1978) 909.
9 C. J. Howard, *J. Chem. Phys., 67* (1973) 5258.
10 P. L. Trevor, J. S. Chang and J. R. Barker, paper presented at *14th Informal Conf. on Photochemistry, Newport Beach, California, April 1980.*
11 R. A. Cox and K. Patrick, *Int. J. Chem. Kinet., 11* (1979) 635.
12 O. Morel, R. Simonaitis and J. Heicklen, *Chem. Phys. Lett., 73* (1980) 38.
13 J. R. Barker, personal communication, 1979.
14 L. T. Molina, S. D. Schinke and M. J. Molina, *Geophys. Res. Lett., 4* (1977) 580.
15 H. Johnston and R. A. Graham, *J. Phys. Chem., 77* (1973) 62.
16 F. Biaume, *J. Photochem., 2* (1973) 139.
17 C. L. Lin, N. K. Rohatgi and W. B. DeMore, *Geophys. Res. Lett., 5* (1978) 113.
18 D. J. Wuebbles, personal communication, 1980.